RES MILITARIS
REVUE EUROPEENNE D ETUDES EUROPEAN JOURNAL OF MILITARY STUDIES
Social Science Journal

Shrinkage Porosity Analysis On Y-Shape Surface Due to Chilled Ductile Iron Casting

By

Justino M. Salsinha
Master Degree Course, Department of Mechanical Engineering, Diponegoro University, Prof. Soedharto Street, Tembalang, Semarang 50275, Indonesia
Corresponding Author Email: martinssalsinha2608@gmail.com

Rusnaldy
Master Degree Course, Department of Mechanical Engineering, Diponegoro University, Prof. Soedharto Street, Tembalang, Semarang 50275, Indonesia

Paryanto
Master Degree Course, Department of Mechanical Engineering, Diponegoro University, Prof. Soedharto Street, Tembalang, Semarang 50275, Indonesia

Natalino Fonseca
Department of Mechanical Engineering, Dili Institute of Technology, Ai-Meti Laran Street, Dili - Timor Leste

Achmad Widodo
Master Degree Course, Department of Mechanical Engineering, Diponegoro University, Prof. Soedharto Street, Tembalang, Semarang 50275, Indonesia

Abstract

One of the surface hardening processes is chill casting. Chill casting is used for surface hardening of nodular cast iron materials. The problem that often occurs in the chill casting method is porosity which is influenced by the fast-cooling rate between the casting object and the mold wall. This study aims to analyze the microstructure, hardness, and porosity that will form on the surface of the Y-shaped specimen after chilled casting. The material used for casting the Y-Shape specimen is nodular cast iron and the chill material is stainless steel plate. The chill is varied with a thickness of 0.2mm and 0.4mm and will be coated on the surface of the sand mold wall then the chill is preheated at a temperature of 700ºC and 900ºC, then pouring is done at a temperature of 1400ºC. The average hardness value on the surface of the specimen is 500HV-900HV, but in the middle area the hardness only reaches 200HV while the microstructure results in the surface layer are cementite and ledeburite phases, but in the middle area ferrite, and perlite are seen surrounding the nodule graphite structure. In the chill-coated area, although the hardness is high, there are micro-porosities and macro-porosities formed randomly.

Keyword — Chilled Casting, Ductile Iron, preheating temperature, shrinkage porosity.

Introduction

In these modern eras, ductile iron is indispensable in the metal casting industry, for casting components, both large and small, such as spare parts for automobiles, trucks, production machines, and so on [1]. Nodular cast iron is superior to other cast irons because of its high ductility, good machining, and can be heat treated to obtain high hardness and toughness [2]. There have been many components of nodular cast iron casting using different methods for surface hardening, although there are methods that require a lot of costs such as surface coating [3], austempered ductile iron process [4]-[5], surface melted by using chromium alloyed [6] and there are also several studies that have used the chilled casting method to harden the surface of the specimen [7]-[9]. The use of chill in the product casting process to harden the surface is a short process and saves costs, the chill material used is a stainless-steel sheet so that this stainless steel plate will diffuse to the surface of the specimen when the molten material is poured into the mold, therefore the chromium element contained inside the stainless steel plate will form on the surface with a very high hardness [10]-[11]. Surface hardening is a manufacturing stage to produce machine components that require high hardness for wear resistance such as gears, camshafts, crankshafts, bearings, and so on. Thus, this stage of manufacturing is very necessary. Although many methods are used for surface hardening and the hardness obtained is very high up to 700-900HV but there are still weaknesses that often occur such as shrinkage defects and porosity defects on the surface. Research has been carried out from [11] that using SS 304 stainless steel plate as a chill material produces high

hardness but they have not investigated cases such as shrinkage defects, porosity defects, expansion defects, and other problems that occur in surface area which is covered with a chill plate. Research by [12] has also used chilled ductile iron casting to harden the surface, they used preheating to the chill plate before pouring, and they explained that the preheating temperature greatly affects the hardness value and the thickness value of the hardness layer, but they have not investigated the defects on the chill-coated surface. Porosity is formed on the surface of the liquid because it is caused by the presence of air bubbles in the casting material [13], this happens because of the high cooling rate on the surface in the solidification stage [14]-[15]. But there is also a cooling rate that is too slow will produce cavities on the metal surface of the casting due to the movement of grains structure to fill the voids unevenly [16]. Based on the above background, we try to make a Y-Shape specimen using the chilled casting method for surface hardening so that we can determine the type of porosity that arises on the surface of the Y-Shape specimen. The purpose of this study is to try to find out what defects occur on the surface of the Y-Shape specimen after the casting process using the chilled casting method in order to increase the surface hardness of the specimen.

Materials And Methodology

The collection of pig iron and steel scrap will be melted at a temperature of 1400^{o}C to produce nodular cast iron. The smelting process uses an electric furnace that has a capacity of 75KVA and an output power of 50W. The crucible capacity is 20kg. Y-Shape pattern made of wood material is shown in Figure 1a, besides that the molding is made of silica sand which is poured into a wooden slab box for the formation of Y-Shape pattern holes, send molding and sample rows can be seen in Figure 1b. The chiller is made of stainless-steel sheet material with type SS 304 and the stainless-steel plate is cut to be attached to the side of the Y-Shape pattern, the dimensions of the Y-Shape pattern, and the position of the chill plate can be seen in Figure 1a. The chill plate thickness is varied into three, namely 0.2mm and 0.4mm. In addition, there

are two variations of the preheating temperature as shown in table 1. The source of fire emitted for preheating is using argon gas and O_2 with a flow speed of 10 liters/minute. Preheating was applied to the step before pouring, two specimens (B1 and B2) used preheating of 700^{o}C while two specimens (B3 and B4) used preheating temperature of 900^{o}C and two other specimens (B5 and B6) did not use preheating as shown in Table 1.

After the Y-Shape specimen casting ends, the next process is cutting the sample for preparation for the micro-Vickers test, microstructure test, and porosity test. The test procedures and test equipment used are the same as those carried out in the study [11], In addition, the position of the test points and the number of test points taken on the surface of the Y-Shape sample which is coated with plate chill are the same except for the porosity test. The position of the test point can be seen in Figure 2.

Table 1 *Chill parameter design to use for coating on Y-Shapes.*

Code of Sample	Chill thickness (SS 304 plates)	Preheating (argon gas and O_2)
B1	0.2 mm	(700^{o}C)
B2	0.4 mm	(700^{o}C)
B3	0.2 mm	(900^{o}C)
B4	0.4 mm	(900^{o}C)
B5	0.2mm	Not heating
B6	0.4mm	Not heating

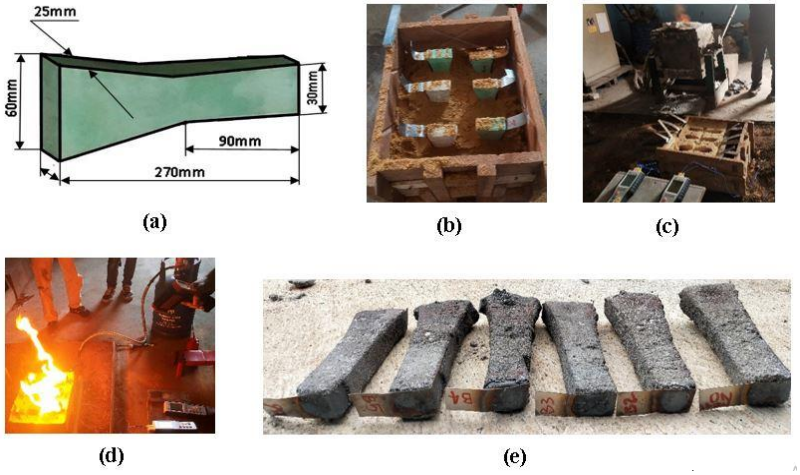

Figure 1 Sample and casting process. (a) Y-Shape pattern and dimensions (b) Y-Shape pattern is installed into the silica sand mold (c) the position of the sand mold and digital thermocouple that is ready for casting (d) preheating process before pouring (e) casting specimen products.

The microstructure test was carried out to determine the phase structure formed on the surface of the specimen and SEM EDX was used to support analyzing the porosity that occurred. If the graphite formed is round and dark, it is a porosity defect. Porosity testing is carried out based on the pycnometer method and in accordance with Archimedes' principles [17] by calculating the weight of the specimen in the air and calculating the weight of the specimen in the water, after that a calculation is carried out using the formula (2) to determine the amount of porosity (%) that occurs on the chill-coated surface.

The actual densities of dry solids (ρ_s) and enclosed water (ρ_{th}) can also be defined [19]:

$$\rho_s = \frac{m_s}{v_s} \text{ (Kg/cm}^3\text{)} \quad \text{..... (1)}$$

Where, ρ_s is apparent density (kg/cm^3), m_s is masses of dry solids and water (kg), v_s is the volume of dry solids water (kg/cm^3).

$$\%P = (1-\frac{\rho_s}{\rho_{th}})x100\% \quad \text{.....(2)}$$

Where ρ is actual density (kg/cm^3), ρ_s is apparent density (kg/cm^3), ρ_{th} is true density (kg/cm^3).

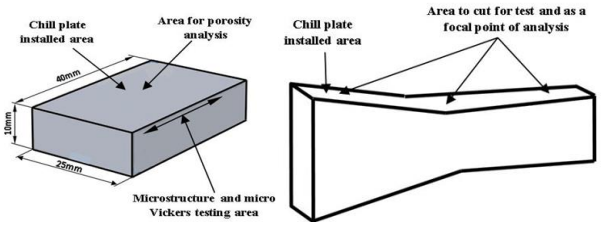

(a) **(b)**

Figure 2 *Specimen for testing (a) position chill plate on the side of Y-Shape product (b) position of test point on the sample after cutting.*

The number of samples for the porosity test was 6 based on the parameters specified in Table 1. However, the number of focal points in each specimen was 16 points for SEM-EDX analysis because three focus points of analysis (Fig 2a) were taken from each specimen (B1, B2, B3, B4, B5, B6). From the three focus points of the analysis, the average value will be taken to fill in the data. Samples for the density test as many as 16 samples and the dimension as shown in Figure 3 were then added together and took the average value to be input into formula 2. Furthermore, the porosity presentation data can be compared with each other.

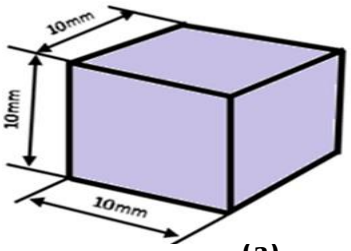

(a)

Figure 3 *the shape and dimension of specimens for density testing*

Results And Discussion

A. Chemical composition

The results of the chemical composition obtained on the nodular cast iron material after casting the Y-Shape product are as follows 3.75%C, 0.47%Mn, 2.03%Si, 0.04%Cr, 0.17%Ni, 0.07%Mo, 0.15%Cu, 0.02%P, 0.15%Ce, 0.06%Mg and the other is Fe, the results of this chemical composition are the same as in previous studies which used the same casting process [12].

B. Microstructure and hardness

The result of the microstructure is ferrite and perlite phases surrounding the spherical graphite which can be seen in Figure 4, this phase is well and evenly formed due to the nodularization or magnesium (Mg) treatment process so that a graphite nodule structure is formed in the middle area for all specimens, but in chill-coated surface area is different. The structure or phase formed in the average surface area is ferrous carbide and is commonly referred to as cementite. The cementite phase is formed because the carbon value contained in the material is more than 2%. The carbon can exist either dissolved in the iron or a combined form, such as iron carbide (Fe_3C). The influence of carbon on the mechanical properties when the carbon content is above 2%, the rigidity and the strength of iron will increase, and its plasticity and toughness will decrease [20]. While on the surface of the Y-Shape specimen there is a chromium structure combined with ferro carbide, the matrix of this structure is the combined form or called Fe-Cr-C.

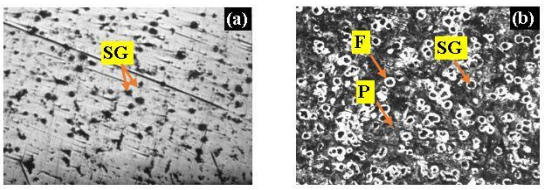

Figure 4 *growth of microstructure in the center zone for all of Y-Shape samples (a) before etching with the zoom scale100x (b) after etching with the zoom scale100x (SG: Spheroidal graphite, F: Ferrite, P: Perlite).*

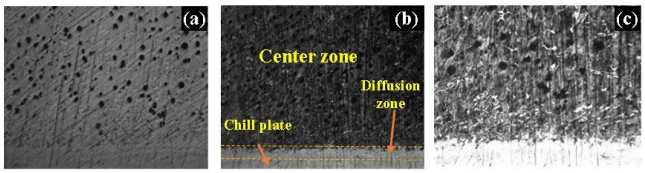

Figure 5 *The sample of B1 (a) before etching with zoom scale 50x (b) after etching with zoom scale 50x (c) after etching with zoom scale 100x (C: Cementite, L: Ledeburite, M: Martensite).*

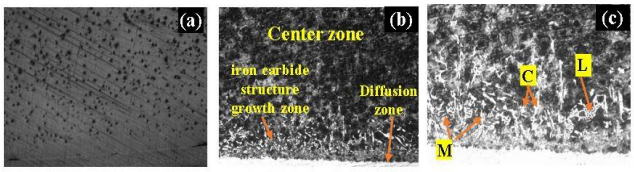

Figure 6 *The sample of B2 (a) before etching with zoom scale 50x (b) after etching with zoom scale 50x (c) after etching with zoom scale 100x (C: Cementite, L: Ledeburite, M: Martensite).*

The result of the microstructure on the surface layer of specimens B1 and B2 is ferro-carbide and in the skin layer or the diffusion zone there is a ledeburite structure. This ledeburite structure is formed due to the diffusion of the chill material used. This ledeburite structure is so hard that its hardness value reaches 900HV as has been investigated by [12] and also research by [11] because the results of their research also use chill, preheating materials and the process is the same. However, sample B1 uses a chill thickness of 0.2mm and a preheating temperature of 700^{o}C, the thicker of the diffusion thickness as seen in Figure 5. In addition, the sample using a chill plate thickness of 0.4mm and then using a preheating temperature of 900^{o}C can be seen in Figure 8, or the number sample of B4 has a thick layer of thick diffusion too.

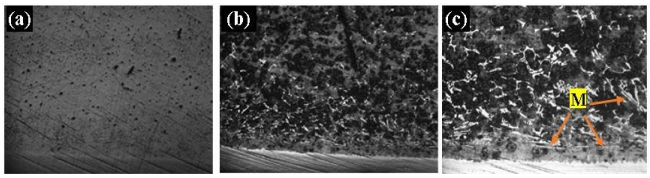

Figure 7 *The sample of B3 (a) before etching with zoom scale 50x (b) after etching with zoom scale 50x (c) after etching with zoom scale 100x (M: Martensite).*

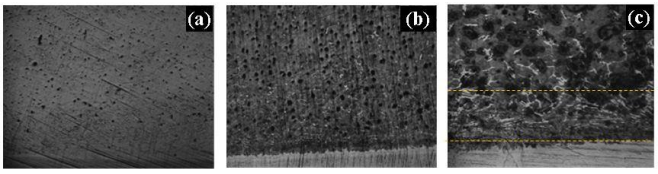

Figure 8 The sample of B4 (a) before etching with zoom scale 50x (b) after etching with zoom scale 50x (c) after etching with zoom scale 100x.

The results for this B4 specimen have a thick layer of hardness because it uses a very thick chill material and also uses a high preheating temperature. The preheating temperature in the diffusion system greatly determines the elements being dislocated from one place to another at the end of solidification. [21].

The structure of the phase formed on the surface of the specimen that does not use preheating such as samples B5 and B6 can be seen in Figure 9 and Figure 10 is the average martensite phase and cementite phase in the area covered with plate chill, this phase is formed due to the fast cooling rate as described by [22] mainly using a chill plate thickness of 0.4mm, the thicker the chill plate is coated on the surface of the mold, the faster the cooling rate is [23].

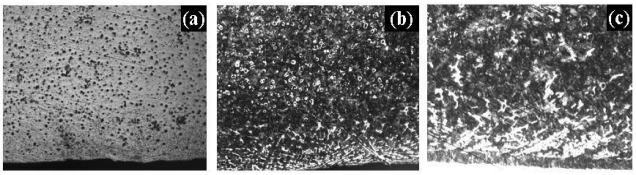

Figure 9 *The sample of B5 (a) before etching with zoom scale 50x (b) after etching with zoom scale 50x (c) after etching with zoom scale 100x.*

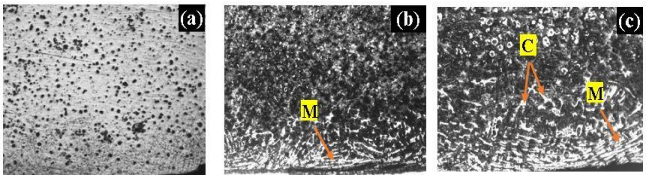

Figure 10 *The sample of B6 (a) before etching with zoom scale 50x (b) after etching with zoom scale 50x (c) after etching with zoom scale 100x (M: Martensite, Cementite).*

This occurs because heat is removed more efficiently from the portions of the casting in contact with the chill than from those in contact with mold components. The value of hardness in samples such as B5 and B6 which have iron carbide or the so-called cementite phase structure is an average of 500HV-700HV as the test results found in previous studies [12]-[11].

C. Porosity test

In general, the case that, the main cause of porosity in the casting results from the evolution of hydrogen or water vapor during solidification. The hydrogen and oxygen contents increase because of enrichment during solidification, as described previously for cast iron. The

main cause of porosity in the casting results from the evolution of hydrogen or water vapor during solidification. The hydrogen and oxygen contents increase because of enrichment during solidification, as described previously for cast iron. The porosity formed on the chill-coated surface after SEM photos were taken is that there are three types of shrinkage porosity, namely microporosity, macroporosity and cave surface. The shape of this porosity defect is not the same. Table 2 shows the results of the porosity presentation value test for specimen B1 but for each specimen, it will be calculated using the same method. Previously, first determine the value of true density and apparent density and calculation data using the method according to the ASTM E-252 standard [24]. Sample B1 uses a chill plate thickness of 0.2mm and uses a preheating temperature of 700^{o}C. It shows that the porosity that occurs on the surface is 5.083%, this value is calculated and can be seen in table 3. That there is not too much macroporosity and there are also pores, namely microporosity as shown in Figure 11a. Slight porosity defects are formed because the cooling rate is slow due to the use of preheating. The porosity for specimen B2 is in the form of micro-porosity and there is also a caved surface as shown in Figure 11b, this caved surface occurs because the bonding structure is not strong, because it uses a chill thickness of 0.4mm, thus the cooling rate is increasing when compared to sample B1. The number of shrinkages porosity formed on the chill-coated surface was 6.141%.

Table 2 *True density calculation data according to ASTM E-252 standard.*

Element diffusion	1/Density (m^3/mg)	Mass (weight %)	1/density x Mass (weight %)
Cr	8.030	6.110	49.063
Fe	8.030	58.150	466.945
O	8.030	18.810	151.044
C	8.030	11.320	90.900
Si	8.030	1.730	13.892
Ni	8.030	1.770	14.213
Mo	8.030	0.010	0.080
Al	8.030	0.120	0.964
Na	8.030	0.350	2.811
Ca	8.030	0.330	2.650
Mg	8.030	0.340	2.730
TOTAL			**72.299**

The value of true density is $\frac{100}{27.299} = 1.383$ g/cm^3, therefore 1.383 g/cm^3, this calculation is for the sample B1, in addition to other samples (B2, B3, B4, B5, and B6) is to use the same calculation to get the total value of the true density. While the apparent density value is to find the mass (grams) and volume (cm^3) for each specimen and calculated by using the formula of number 1. So it will determine the value of the presentation of the total porosity. The total value of porosity can be seen in Table 3.

Table 3 *total value of shrinkage porosity after calculation using formula 2 and based on the*

Sample code	True density (g/cm^3)	Apparent density (g/cm^3)	Shrinkage porosity (%)
B1	1.383	8.030	5.083
B2	1.148	8.050	6.141
B3	1.163	8.040	6.053
B4	1.388	8.050	5.079
B5	1.009	8.080	7.017
B6	1.060	8.090	6.689

Furthermore, the sample of B3 using a chill plate thickness of 0.2mm and using preheating, micro and macroporosity have been detected on the surface of the area coated by the chill plate, which can be seen in Figure 11c. However, by using the preheating process at high temperatures, the shrinkage porosity has a value of 6.053% which can be seen in table 3. On the other hand, the chromium element is visible that has diffused to the surface of the ductile iron specimen.

Sample B4 is that there are only slight pores along the chill-coated area as shown in Figure 12a, the type of defect is microporosity which has a shrinkage porosity value of 5.079% which can be seen in Table 3. Due to the higher preheating temperature, the slower the cooling rate on the surface.

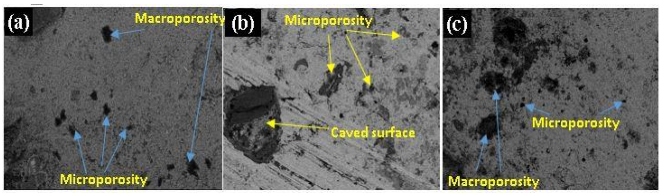

Figure 11 *surface analysis by using SEM-EDX to find the shrinkage porosity with the scale zoom 100x (a) sample of B1 (b) the sample of B2 (c) the sample of B3.*

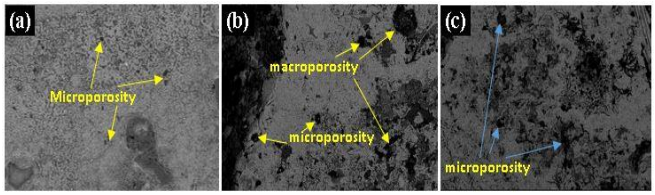

Figure 12 *surface analysis by using SEM-EDX to find the shrinkage porosity with the scale zoom 100x (a) sample of B4 (b) the sample of B5 (c) the sample of B6.*

Porosity occurs in specimens that do not use preheating, the average porosity is microporosity and macroporosity can be seen in Figures 11b and 11c. Because the plate chill used produces a very high cooling rate, air bubbles form on the chill-coated surface. The porosity defect found on the surface of sample B5 was 7.017% (Fig 12b), besides that the microporosity for sample B6 was equal to 6.689% which can be seen in Figure 12c.

Micro and macroporosity are formed because it is influenced by several factors such as fast cooling rate, poor riser design, and also very low pouring temperature, resulting in slower dendritic structure growth resulting in pores forming between the cell gaps of the matrix structure in solid materials. [25]. Another cause is that the cooling rate between the cast and molded material is too high [15].

Iv Conclusions

From the results of the research that has been discussed about microstructure, hardness, and shrinkage porosity which uses variations in the thickness of the chill used and variations in temperature used, the researchers want to draw the following conclusions:

1. By using a chill made of stainless steel SS 304 material, ferro carbide was formed and the cementite structure grew in the chill-coated surface area. This cementite structure is very hard, the hardness value reaches 900HV.
2. Using the preheating process on plate chill before casting, greatly affects the growth of ferrous carbide and cementite phase. The higher the preheating temperature, the ferro

carbide structure formed is not too broad and the cementite structure is well-formed due to the presence of diffused elements, while the shrinkage porosity is reduced.

3. Using a chill plate thickness of 0.4mm and a high preheating temperature, the shrinkage porosity decreases.
4. Without using the preheating process on the chill plate, the shrinkage porosity increases, even though there is a large amount of martensite on the surface.

Acknowledgments

The study was carried out with partial financial support provided by the Diponegoro University Scholarship Prof. Soedharto Street, Tembalang, -Semarang 50275, Indonesia. We also thank to Diponegoro University Semarang-Indonesia and Politeknik Manufacture Ceper Klaten-Indonesia for supporting the laboratory of testing.

References

L. M. Robert, “Machine Element in Mechanical Design,” Fouth Edit. New Jersey Columbus, Ohio: Pearson Prentice Hall, 2004.

J.R. Davis, Gear Materials, Properties, and Manufacture. ASM International, 2005.

H. T. Cao et al, “Surface alloying of high-vanadium high-speed steel on ductile iron using plasma transferred arc technique: Microstructure and wear properties,” vol. 100, pp. 223–234, 2016.

S. Samaddar, T. Das, A. K. Chowdhury, and M. Singh, “Manufacturing of Engineering components with Austempered Ductile Iron - A Review,” Mater. Today Proc., vol. 5, no. 11, pp. 25615–25624, 2018.

M. H. Sohi, G. Karshenas, and S. M. A. Boutorabi, “Electron beam surface melting of as-cast and austempered ductile irons,” Mater. Process. Technol., vol. 153–154, pp. 199–202, 2004.

M. H. Sohi, M. Ebrahimi, H. M. Ghasemi, and A. Shahripour, “Microstructural study of surface melted and chromium surface alloyed ductile iron,” Appl. Surf. Sci., vol. 258, no. 19, pp. 7348–7353, 2012.

J. C. Ferreira, “A study of cast chilled iron processing technology and wear evaluation of hardened gray iron for automotive application,” J. Mater. Process. Technol., vol. 121, no. 1, pp. 94–101, 2002.

K. Kanthavel, K. Arunkumar, and S. Vivek, “Investigation of chill performance in a steel casting process using Response Surface Methodology,” Procedia Eng., vol. 97, pp. 329–337, 2014.

L. C. Kumruoğlu, “Mechanical and microstructure properties of chilled cast iron camshaft: Experimental and computer-aided evaluation,” Mater. Des. vol. 30, no. 4, pp. 927–938, 2009.

M. Qian, S. Harada, Y. Kuroshima, and H. Nagayoshi, “Surface hardening of ductile cast iron using stainless steel,” Mater. Sci. Eng. A, vol. 208, no. 1, pp. 88–92, 1996.

N. F. D. S. Guterres, Rusnaldy, A. Widodo, and T. Carwita, “The effect of chills thickness to microstructure and surface hardness layer on specimen ductile cast iron,” 4Th Int. Conf. Mater. Metall. Eng. Technol., vol. 2384, no. December, p. 040004, 2021.

N. F. D. S. Guterres, Rusnaldy, A. Widodo, and A. Syamsudin, “Investigate Temperature Preheating on the Chill Plate to Identify Surface Characteristic on the Ductile Iron by Sand Casting,” Int. J. Eng. Mater. Manuf., vol. 6, no. 3, pp. 141–151, 2021.

B. Richard Gundlach, “Metals Handbook. Vol. 15, 9th ed. ASM International, 1988.

D. Szeliga, "Manufacturing of thin-walled Ni-based superalloy castings using an alternative thermal insulating module to control solidification," J. Mater. Process. Technol., vol. 278, p. 116503, 2020.
J. Beddoes and M. J. Bibby, "Principles of Metal Manufacturing Processes". Canada: Elsevier, 2003.
H. Steve, "Metal Casting Appropriate technology in the small foundry". London-UK: Intermediate Technology Publications Ltd, 1996.
R. P. Taylor, S. T. McClain, and J. T. Berry, "Uncertainty analysis of metal-casting porosity measurements using Archimedes' principle," Int. J. Cast Met. Res., vol. 11, no. 4, pp. 247–257, 1999.
D. A. Tyagita and A. Irawan, "Porosity and Microstructure Analysis in Aluminum Waste Pieces," pp. 565–571, 2018.
N. P. Zogzas, Z. B. Maroulis, and D. Marinos-Kouris, "Densities, shrinkage and porosity of some vegetables during air drying," Dry. Technol., vol. 12, no. 7, pp. 1653–1666, 1994.
A. Kahyarian "CO_2 corrosion of mild steel Iron Carbide (Fe_3C)," in Book Section, pp. 2–56, 2017.
J. D. G. R. William D. Callister, Material Science and Engineering an Introduction, Eight editions. United State of America: John Wiley & Sons, Inc., 2010.
R. A. Flinn, Metals Handbook. Vol. 15. United State of America, 1988.
R. D. Sulamet-Ariobimo, J. W. Soedarsono, and B. Suharno, "Cooling Rate Analysis of Thin Wall Ductile Iron Using Microstructure Examination and Computer Simulation," Appl. Mech. Mater., vol. 752–753, pp. 845–850, 2015.
ASTM E-252, E252-06 Standard Test Method for Thickness of Foil, Thin Sheet, and Film by Mass Measurement, vol. 06, no. Reapproved. 2013.
S. N. Lekakh and B. Hrebec, "Solidification kinetics of graphite nodules in cast iron and shrinkage porosity," Int. J. Met., vol. 10, no. 4, pp. 389–400, 2016.